

1 **Contrasting Rhizosphere Nitrogen Dynamics in Andropogoneae Grasses: Implications for**  
2 **Sustainable Agriculture**

3

4 Sheng-Kai Hsu<sup>1\*</sup>, Bryan D Emmett<sup>2</sup>, Alexandria Haafke<sup>2</sup>, Germano Costa-Neto<sup>1</sup>, Aimee J  
5 Schulz<sup>3</sup>, Nicholas Lepak<sup>4</sup>, Thuy La<sup>1</sup>, Taylor AuBuchon-Elder<sup>5</sup>, Charles Hale<sup>3</sup>, Sierra S Raglin<sup>6</sup>,  
6 Jonathan O Ojeda-Rivera<sup>1</sup>, Angela D Kent<sup>6,7</sup>, Elizabeth A Kellogg<sup>5,8</sup>, M Cinta Romay<sup>1</sup> and  
7 Edward S Buckler<sup>1,3,4\*</sup>

8

9 <sup>1</sup>Institute for Genomic Diversity, Cornell University, Ithaca, NY, USA 14853

10 <sup>2</sup>USDA-ARS, National Laboratory for Agriculture and the Environment, Ames, IA, USA 50011

11 <sup>3</sup>Section of Plant Breeding and Genetics, Cornell University, Ithaca, NY USA 14853

12 <sup>4</sup>USDA-ARS, Robert W. Holley Center for Agriculture and Health, Ithaca, NY, USA 14853

13 <sup>5</sup>Donald Danforth Plant Science Center, St. Louis, MO, USA 63132

14 <sup>6</sup>Carl R. Woese Institute for Genomic Biology, University of Illinois at Urbana-Champaign,  
15 Urbana, IL, USA 61801

16 <sup>7</sup>Department of Natural Resources and Environmental Sciences, University of Illinois at Urbana-  
17 Champaign, Urbana, IL, USA 61801

18 <sup>8</sup>Arnold Arboretum of Harvard University, Boston, MA, USA 02130

19 \*Correspondence: Sheng-Kai Hsu, [sh2246@cornell.edu](mailto:sh2246@cornell.edu); Edward S Buckler, [esb33@cornell.edu](mailto:esb33@cornell.edu)

20

21 **Summary**

22 **Background:** Nitrogen (N) fertilization in crop production significantly impacts ecosystems, often  
23 disrupting natural plant-microbe-soil interactions and causing environmental pollution. Our  
24 research tested the hypothesis that phylogenetically related perennial grasses might preserve  
25 rhizosphere management strategies conducive to a sustainable N economy for crops.

26

27 **Method:** We analyzed the N cycle in the rhizospheres of 36 Andropogoneae grass species related  
28 to maize and sorghum, investigating their impacts on N availability and losses. This assay is  
29 supplemented with the collection and comparison of native habitat environment data for ecological  
30 inference as well as cross-species genomic and transcriptomic association analyses for candidate  
31 gene discovery.

32

33 **Result:** Contrary to our hypothesis, all examined annual species, including sorghum and maize,  
34 functioned as N "Conservationists," reducing soil nitrification potential and conserving N. In  
35 contrast, some perennial species enhanced nitrification and leaching ("Leachers"). Yet a few other  
36 species exhibited similar nitrification stimulation effects but limited  $\text{NO}_3^-$  losses ("Nitrate  
37 Keepers"). We identified significant soil characteristics as influential factors in the eco-  
38 evolutionary dynamics of plant rhizospheres, and highlighted the crucial roles of a few transporter  
39 genes in soil N management and utilization.

40

41 **Conclusion:** These findings serve as valuable guidelines for future breeding efforts for global  
42 sustainability.

43

44 **Key words:** Rhizosphere, Nitrogen Cycle, Andropogoneae, Sustainability, Evolution

## 45 **Introduction**

46 The development of inorganic nitrogen (N) fertilizer has revolutionized modern agriculture  
47 (Khush, 2001; Smith *et al.*, 2020). Nevertheless, the benefit comes at the cost of severe  
48 environmental impacts. The soil microbial processes of nitrification and denitrification, which  
49 transform the less mobile ammonium ( $\text{NH}_4^+$ ) into free nitrate ( $\text{NO}_3^-$ ) and nitrite ( $\text{NO}_2^-$ ), lead to  
50 inefficient use of synthesized inorganic N on farms and environmental pollution (Bremner &  
51 Blackmer, 1978; Schlesinger, 2009; Billen *et al.*, 2013).  $\text{NO}_3^-$  leaches from agricultural soil,  
52 leading to eutrophication of neighboring water systems (Schlesinger, 2009; Billen *et al.*, 2013).  
53 The hypoxic zone in the Gulf of Mexico serves as a cautionary example (Rabalais & Turner, 2019).  
54 Soil nitrous oxide ( $\text{N}_2\text{O}$  and  $\text{NO}_x$ ) emission accounts for ~60% of agricultural greenhouse gas  
55 footprint:  $\text{N}_2\text{O}$  exhibits 265 times higher global warming potential than  $\text{CO}_2$ , and 75% of  
56 anthropogenic  $\text{N}_2\text{O}$  emission in the US is from nitrification and denitrification processes in  
57 agricultural soils (EPA, 2023). N loss from agricultural soils is particularly evident in early spring  
58 (Lu *et al.*, 2022), likely due to the mismatch in timing between crop fertilization, plant N demand,  
59 and soil microbial activities (Supplementary Figure S1; Bender *et al.*, 2013; Hartman *et al.*, 2022;  
60 Kosola *et al.*, 2023). Therefore, ensuring early, efficient and conservative utilization of soil N on  
61 farms is crucial for global sustainability.

62  
63 Recently, Subbarao & Searchinger, 2021 proposed a “more ammonium solution,” which  
64 emphasizes managing soil nitrification rates to conserve N as  $\text{NH}_4^+$  in the soil. The proposed  
65 approach requires careful and precise orchestration of the three-way interactions among plants,  
66 soil and microbes. Soil characteristics, such as moisture and pH, affect plant growth, microbial  
67 activity, and their interactions, including competition and various symbiotic relationships  
68 (McNear, 2013). Conversely, microbes and plants can also modify soil properties to benefit their  
69 own growth (McNear, 2013). Given the complexities of plant-soil-microbe interactions, it is not  
70 entirely clear whether and how to control nitrification in agricultural soil.

71  
72 Previous efforts have focused on plants and their impact on rhizosphere microbes. Crop scientists  
73 identified the biological nitrification inhibition (BNI) capacity in various crops (Subbarao *et al.*,  
74 2007c, 2009, 2013; Pariasca Tanaka *et al.*, 2010; Tesfamariam *et al.*, 2014; Sun *et al.*, 2016; Byrnes  
75 *et al.*, 2017; Nuñez *et al.*, 2018; Villegas *et al.*, 2020), with the goal of improving their ability to

76 inhibit soil nitrification on farms. Significant advances were made in identifying root exudates  
77 with nitrification-inhibiting effects and understanding their biosynthesis (Tesfamariam *et al.*,  
78 2014; Widhalm & Rhodes, 2016; Wang *et al.*, 2020; Pan *et al.*, 2021; Otaka *et al.*, 2022). More  
79 recently, a few studies have started to investigate the genetic variation within crop species to  
80 explore the potential of genetic improvement (Petroli *et al.*, 2023) and between species to seek  
81 transferable BNI-contributing alleles from wild relatives (Subbarao *et al.*, 2007b, 2021).

82  
83 However, the benefit of BNI capacity in a crop species could vary depending on its  $\text{NH}_4^+$  uptake  
84 efficacy (Abalos *et al.*, 2018) and its tolerance to  $\text{NH}_4^+$  toxicity (Esteban *et al.*, 2016). There is  
85 massive variation in the preference between  $\text{NH}_4^+$  and  $\text{NO}_3^-$  among plant species adapted to distinct  
86 environments (Houlton *et al.*, 2007; Kahmen *et al.*, 2008; Boudsocq *et al.*, 2012; Britto &  
87 Kronzucker, 2013). Hence, it is conceivable that suppression of nitrification can be detrimental to  
88  $\text{NO}_3^-$ -preferring species (Boudsocq *et al.*, 2012; Konaré *et al.*, 2019) and the nitrification process  
89 is not necessarily harmful to the environment if the converted  $\text{NO}_3^-$  can be efficiently assimilated  
90 and utilized. For instance, even within species, two ecotypes with opposing effects on nitrification  
91 were found in different sites for *Hyparrhenia diplandra* (Lata *et al.*, 2000). We hypothesize that  
92 diverse species adapting independently to various environments manage their rhizosphere  
93 differently, resulting in divergent patterns of N-cycling. Amongst the range in rhizosphere N  
94 dynamics across species, we seek alternative strategies for N conservation in agricultural soils. In  
95 particular, we anticipate finding favorable phenotypes among perennial grasses that establish  
96 earlier in the season than the annual crops.

97  
98 In this study, we focus on the Andropogoneae tribe of grasses, which has evolved to dominate 17%  
99 of global land area with C4 photosynthesis, adapting to diverse habitats, often forming large  
100 populations (Moore *et al.*, 2019; Cowan *et al.*, 2020; Bachle *et al.*, 2022). Importantly, maize, one  
101 of the most productive crops on earth, belongs to this tribe. We carried out a systematic assay on  
102 the rhizosphere N traits in 36 Andropogoneae species, including maize and sorghum, during their  
103 active vegetative growing stage. We discovered pronounced phenotypic variation and identified  
104 three distinct rhizosphere N management strategies amongst different species:  $\text{NH}_4^+$  conservation,  
105  $\text{NO}_3^-$  leaching, and  $\text{NO}_3^-$  retention. Further biogeographical and environmental association  
106 provides insights into the ecological selection forces shaping the three strategies. Through cross-

107 species genomic/transcriptomic association analysis, we identified key genes and breeding targets  
108 that could enhance agricultural sustainability.

109

## 110 **Materials and Methods**

### 111 **Plant materials**

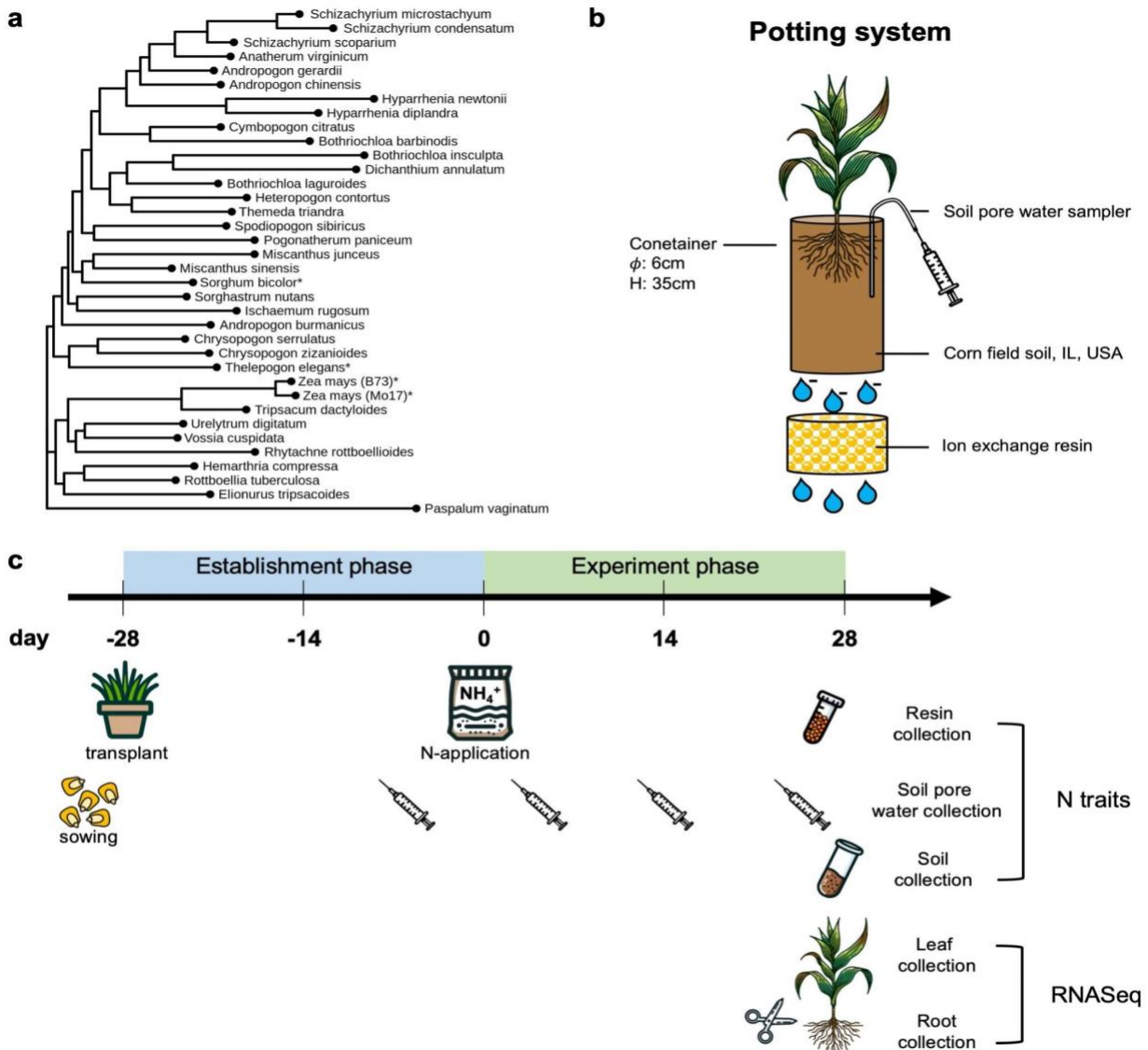
112 In this study we investigate a total of 36 Andropogoneae species, including two important annual  
113 crops: maize (*Zea mays*) and sorghum (*Sorghum bicolor*) (Supplementary Table S1). These 36  
114 species are distributed across the Andropogoneae phylogeny (Figure 1a). Significant BNI effect  
115 was shown in maize and sorghum previously (Subbarao *et al.*, 2013; Otaka *et al.*, 2022; Petroli *et*  
116 *al.*, 2023). Except for maize and sorghum (seeds produced in the lab nursery), live clones of the  
117 other 34 species were either clonally propagated from wild grassland habitats or grown from seeds  
118 obtained from wild collections, the USDA-ARS National Plant Germplasm System, Iowa State  
119 University, or commercial sources (Supplementary Table S1). Plant materials were clonally  
120 propagated in a greenhouse with 14 hours of daylight at 28°C and 10 hours of nighttime at 22°C.  
121 Supplemental lights turned on when natural light was below 500 W/m<sup>2</sup>. Soil moisture was  
122 maintained by daily watering. The plants were fertilized three times a week during watering  
123 (480ppm 21-5-20: 7.92% NH<sub>4</sub><sup>+</sup> and 13.08% NO<sub>3</sub><sup>-</sup>; 1350ppm 15-5-15 + 4% Ca + 2% Mg: 3% NH<sub>4</sub><sup>+</sup>  
124 and 12% NO<sub>3</sub><sup>-</sup>; 300ppm Fe chelate).

125

### 126 **Greenhouse experiment**

127 We performed a greenhouse experiment to investigate the phylogenetic variation of the  
128 rhizosphere N cycle across Andropogoneae. This experiment followed a complete randomized  
129 design (CRD) with three replicates per species. Greenhouse condition was the same as the  
130 maintenance. For mesocosm soil, we used a 1:4 mixture of US corn belt soil (sourced from IL,  
131 USA, 40.05180278°N 88.23133889°W; Soil features: OM 3.0%, CEC 16.4 meq/100g, pH 6.9,  
132 NO<sub>3</sub><sup>-</sup> 5.9 ppm, NH<sub>4</sub><sup>+</sup> 2.5 ppm, P 22 ppm, K 109 ppm) and Cornell Potting mix (a premix of 3.8 ft<sup>2</sup>  
133 peat, 4 ft<sup>2</sup> vermiculite, 4 ft<sup>2</sup> perlite, 50 lbs turface, 3 lbs limestone, 4 lbs 10-5-10 Media Mix  
134 fertilizer, and 2 lbs calcium sulfate). Maize and sorghum were germinated and grown for two  
135 weeks. Then, seedlings of maize and sorghum and clonal plantlets of other species were  
136 transplanted to cylindrical containers (diameter of 6 cm and height of 35 cm) filled with 700g of  
137 mesocosm soil (Figure 1b). The clonal plantlets were trimmed to 15cm above soil to promote  
138 regrowth. After transplantation, we allowed a 4-week establishment period with regular nutrient  
139 supply as in the maintenance protocol. Afterward, a one-time application of 150 kg/ha NH<sub>4</sub><sup>+</sup>-N as  
140 (NH<sub>4</sub>)<sub>2</sub>SO<sub>4</sub> (1000 ppm N) initiates the formal experiment (Figure 1c). At the end of the

141 establishment period, fine nylon mesh bags containing 400ml of ion exchange resins (MAG-MB,  
142 Resintech) are placed under the containers to capture leached  $\text{NO}_3^-$  from the system, and Rhizon  
143 soil moisture samplers (Eijkelkamp Agrisearch Equipment) were installed for soil pore water  
144 sampling (Figure 1b). After transplantation, we irrigated each plant with 100ml of water daily to  
145 control for the leaching rate. We collected soil pore water samples on day -4, 3, 15, 24 of the  
146 experiment (Figure 1c). Sampling is conducted an hour after irrigation of 100ml water by suction  
147 pressure using a common medical syringe via the Rhizon samplers. A sample of 10 ml of soil  
148 solution was collected and stored at  $-20^\circ\text{C}$  for later assay. On day 27, resin traps were collected  
149 (Figure 1c). The resin was thoroughly homogenized and an aliquot of 40 ml resin of each bag was  
150 sampled and stored at  $4^\circ\text{C}$ . On day 28, we collected root (5cm from the tips), leaf (5cm from the  
151 tips) and soil samples (Figure 1c). Two samples of 40ml sieved soil per replicate were collected  
152 and stored at  $4^\circ\text{C}$ : one for  $\text{NO}_3^-$  extraction and one for potential nitrification rate measurement.  
153 Both collected soil and resin samples were processed within 14 days after the sampling.  
154



155

156 **Figure 1. Plant materials and experimental design**

157 **a.** Phylogenetic tree of the Andropogoneae grass species studied in the study. Asterisks denote annual taxa. **b.**

158 Illustration of the potting setup. Each seedling is planted in a tall cylindrical pot with a height (H) of 35cm and a

159 diameter ( $\phi$ ) of 6cm. A soil pore water sampler is inserted to the soil and a trap with ion-exchange resins is installed

160 beneath the pot. **c.** Timeline of the greenhouse experiment. There are four weeks of establishment phase for the plant

161 to recover from the transplantation. The experiment starts with the application of 150 kg/ha  $\text{NH}_4^+\text{-N}$  as  $(\text{NH}_4)_2\text{SO}_4$

162 (1000 ppm N). We collect soil pore water samples on day -4, 3, 15, 24 of the experiment. On day 27, resin traps are

163 collected. On day 28, we collected soil samples and plant tissues. Soil pore water, resin and soil samples are for

164 rhizosphere N trait measurement and the plant tissues are subjected to RNA extraction and sequencing.

165

166

167 **NO<sub>3</sub><sup>-</sup> extraction and quantification**

168 We extracted 2 grams of fresh soil media in 5 ml of 2M KCl extraction solution. The samples were  
169 shaken for 1 hour. After shaking, the samples were allowed to rest undisturbed for at least 30  
170 minutes. The top layer of the extract solution, in a volume greater than 1 ml, was then filtered into  
171 new tubes. Similarly, for resin extraction, we extracted 2 grams of resin in 5 ml of 2M KCl. The  
172 extracts were stored at -80°C until shipment and quantification. Nitrate concentrations in pore  
173 water, soil and resin extracts were quantified colorimetrically using the VCl<sub>3</sub>/Griess method  
174 (Miranda *et al.*, 2001) in a 96-well microplate (Doane & Horwáth, 2003). Plates were incubated  
175 overnight in the dark and absorbance at 540 nm read using a Synergy HT microplate reader. A  
176 standard curve of 0 to 15 ppm was included on each plate and calculated concentrations expressed  
177 on a soil dry weight basis (µg N g soil<sup>-1</sup>).

178

179 **Potential nitrification rate measurement**

180 Nitrification potential of mesocosm soil was assessed on fresh soils within a week of sampling  
181 using the shaken slurry method of (Hart *et al.*, 1994). Approximately 5 g of moist soil media was  
182 placed in a half pint mason jar along with 33 ml of buffer (0.3 mM KH<sub>2</sub>PO<sub>4</sub>, 0.7 mM K<sub>2</sub>HPO<sub>4</sub>,  
183 0.75 mM (NH<sub>4</sub>)SO<sub>4</sub>, pH 7.2), capped with a vented lid and shaken at 150 rpm at 30 °C for 24 hr.  
184 At 2, 4, 22 and 24 hr a 1 ml aliquot was sampled from each jar and centrifuged at 16,000 x g at  
185 4°C for 10 min, the supernatant removed and stored at -20°C until quantification of nitrate as  
186 described above. Potential nitrification rate (PNR) was calculated as the rate of nitrate  
187 accumulation over time using the equation:

188

189 
$$PNR (mg N kg^{-1} hr^{-1}) = \frac{Rate (mg N L^{-1} hr^{-1}) * 0.033 L + vol. water in soil sample}{kg oven dry soil in jar}$$

190

191 Comparing the PNR of each sample to bulk soil blank samples, we calculated the relative PNR in  
192 percentage as following:

193

194 
$$Relative PNR (\%) = \frac{(PNR_{sample} - PNR_{bulk soil})}{PNR_{bulk soil}}$$

195

## 196 **Characterization of species with distinct rhizosphere N managing strategies**

197 Comparing the average rhizosphere N trait measures of each species to the average measures of  
198 bulk soil blank samples, we identified three groups of species that manage their rhizosphere N  
199 differently. The groups and criteria are as following:

- 200 1) Conservationists: PNR reduced by 25% or more and  $\text{NO}_3^-$  lost by <50%
- 201 2) Leachers: PNR elevated by 25% or more and  $\text{NO}_3^-$  lost by >50%
- 202 3) Nitrate keepers: PNR elevated by 25% or more but  $\text{NO}_3^-$  lost by >50%

203

## 204 **Characterization of geographic adaptation and environmental vectors (envPCs)**

205 To estimate the natural environmental conditions in which each species occurs, we conducted a  
206 two-step environmental characterization. The initial step estimated the geographic range of each  
207 species using geographic coordinates sourced from species diversity and global distribution  
208 databases. This was accomplished using the R packages ‘BIEN’ v1.2.6 (Maitner, 2023) to access  
209 the Botanical Information and Ecology Network (BIEN). Then, the second step was focused on  
210 obtaining the environmental features characteristic of their adaptation. For each coordinate sample,  
211 we extracted a set of 94 environmental factors from diverse publications (Ross *et al.*, 2018;  
212 Lembrechts *et al.*, 2022) and databases, including WorldClim (Fick & Hijmans, 2017), FAO-  
213 GAEZ (‘GAEZ v4 Data Portal’) and GDSE (Shangguan *et al.*, 2014) (Supplementary Table S2)  
214 using the packages ‘terra’ v1.7 (Hijmans *et al.*, 2023). Subsequently, we computed the ranges of  
215 these environmental features for each species in terms of quantiles (10%, 50%, and 90%) across  
216 their geographic distribution. A total of 282 environmental features (a combination of  
217 environmental factors and quantiles) were obtained (Supplementary Table S3). Data quality  
218 control was performed by removing features with a rate of missing values higher than 10%, and  
219 imputing missing values using the function `imputePCA()` from the package ‘missMDA’ v1.19  
220 (Husson & Josse, 2023). Finally, using the function `PCA()` from the package ‘FactoMineR’ v2.9  
221 (Husson *et al.*, 2023), we did an eigen decomposition of the environmental relationship matrix to  
222 obtain linear and orthogonal combinations of numerous environmental features, the so-called  
223 environmental principal components (envPCs; Supplementary Table S3). We assumed that each  
224 envPC captures a different spatial and climatic trend of the global environmental diversity, serving  
225 as a proxy for the ecological range and the selection pressure that might shape the local-adaptation  
226 of each species.

227

## 228 **Association between habitat environment and rhizosphere N traits**

229 To investigate the potential ecological selection pressure that shapes the distinct rhizosphere N  
230 dynamics in Andropogoneae species, we modeled the impact of different environmental features  
231 of the native habitat range on the rhizosphere N traits (i.e. potential nitrification rate, soil NO<sub>3</sub><sup>-</sup>  
232 content, and NO<sub>3</sub><sup>-</sup> loss) as follows:

$$233 \quad Y \sim envPC + \varepsilon$$

234 Where Y stands for average trait values, LoF denotes the binary scores that predict potential  
235 functional loss of the homolog, and  $\varepsilon$  is the residual.

236

237 Using a linear regression approach, we identified the envPCs that significantly co-vary with at  
238 least one rhizosphere N trait (p-value < 0.05). For each significant envPC, we extracted the  
239 significantly contributing environmental features and investigated the distribution of these  
240 variables in the three species groups.

241

## 242 **Genome assemblies**

243 25 of the studied taxa have high quality long read assemblies available publicly (*Zea mays ssp.*  
244 *mays* var. B73 (Hufford *et al.*, 2021), *Zea mays ssp. mays* var. Mo17 (Sun *et al.*, 2018), *Sorghum*  
245 *bicolor* var. Btx623 (v3) (McCormick *et al.*, 2018), *Miscanthus sinensis* (Mitros *et al.*, 2020),  
246 PanAnd (In prep.)). For 9 of the remaining species, short-read whole genome sequencing data were  
247 generated to supplement the long-read data. DNA was extracted from leaves. (Qiagen Inc.,  
248 Germantown, MD). Extracted samples were quantified and Illumina Tru-Seq or nano Tru-seq  
249 libraries were constructed according to sample concentration. Samples were sequenced in pools of  
250 24 individuals in one lane of an S4 flowcell in an Illumina Novaseq 6000 System with 150 bp pair-  
251 end reads. With short sequencing reads passing our customized quality control (Schulz *et al.*,  
252 2023), assemblies were generated using Megahit v1.2.9 (Li *et al.*, 2015) using a minimum kmer  
253 size (--k-min) of 31 and default setting for the other parameters (Schulz *et al.*, 2023). Two studied  
254 genomes without genome assemblies were excluded for phylogenetic and cross-species  
255 association analysis.

256

257

## 258 **Identification of the functional homolog**

259 As the unit of the cross-species genomic and transcriptomic association analyses, we identified the  
260 most likely functional homologous genes among genome assemblies of various Andropogoneae  
261 taxa, using the closest outgroup, seashore paspalum (*Paspalum vaginatum*) (Sun *et al.*, 2022) as  
262 reference. Annotated proteins in seashore paspalum were queried against all Andropogoneae  
263 genomes using miniProt v0.10 (Li, 2023). We retained the primary alignment (with the least  
264 sequence divergence from reference) in each genome to represent the functional homologs. We  
265 studied the functional homologs instead of the syntenic orthologs to prevent the comparison among  
266 orthologs that underwent differential genome contraction processes following whole genome  
267 duplication and/or polyploidization events, which occur repeatedly within the Andropogoneae  
268 tribe (Estep *et al.*, 2014; Mitros *et al.*, 2020; Zhang *et al.*, 2024). Ideally, the functional homologs  
269 represent the most conserved gene copies among the homeologs/paralogs for each species.  
270 Multiple sequence alignments (MSAs) of the coding sequences (CDS) of each functional homolog  
271 were generated using MAFFT v7.508 (Katoh *et al.*, 2002).

272

## 273 **Phylogenetic tree construction**

274 We used the diversity of the putatively neutral loci to construct the phylogenetic relationship  
275 amongst the assayed species in this study. We used the four-fold degenerate sites in the CDS MSA  
276 of 2,000 random homologs that are present in >75% of all assayed species to construct the  
277 maximum likelihood species tree using RAxML v8.2.12 (Stamatakis, 2014) with the GTR model  
278 + Gamma correction for rate heterogeneity (-m GTRGAMMA).

279

## 280 **Loss of function prediction**

281 Assuming functional constraint, for a homolog, we inferred that taxa with no alignment or  
282 unusually long genetic distance to the outgroup (one standard deviation away from average genetic  
283 distance) likely lost or shifted their function. Hence, we define a binary loss-of-function (LoF)  
284 score to represent the presence of a functional gene copy in each taxon. LoF score equals 0 for the  
285 taxa with missing or distant alignments while 1 for the other taxa.

286

287

288

## 289 **RNA extraction and sequencing**

290 RNA was extracted from leaf or root tissues using the Direct-zol-96 RNA extraction kit by Zymo  
291 Research and RNeasy Plant mini kit by Qiagen based on manufacturers' protocols. A few random  
292 RNA samples were selected for fragment analysis using the BioAnalyzer to check for fragment  
293 size and purity using RIN number of >6. RNA-seq library preparation was performed using the  
294 NEBNext® Ultra II Directional RNA Prep Kit for Illumina and NEBNext® Poly(A) mRNA  
295 Magnetic Isolation Module. Initial RNA concentration for each sample used ranged from 250-  
296 1000ng. Pair-end 150bp reads were generated by the Illumina NovaSeq X Plus PE150 platform.

297

## 298 **Homolog expression quantification and normalization**

299 Using Salmon v1.10.2 (Patro *et al.*, 2017), we quantified the expression level of each homolog in  
300 different species in reference to the phylogenetically closest long-read genomes (Supplementary  
301 Table S1). In addition to coding exons of each homolog, we included reads mapped to putative  
302 untranslated regions (within 500bp up- and downstream of the coding regions) for expression  
303 quantification. Libraries with mapping rate < 40% were excluded from the subsequent analyses.  
304 With a consistent set of homologs, expression was quantified in transcripts per million (TPM) and  
305 thus was comparable across species. Only homologs expressed (TPM > 1) in > 10% of samples  
306 were retained for subsequent association analysis. For each taxon, we calculated the average  
307 expression of homologs among the replicates.

308

## 309 **Cross-species genomic and transcriptomic association analyses**

310 To tackle the genetic variation of the rhizosphere N traits amongst the assayed species, we modeled  
311 the trait variation with the functionality and regulation of each homolog separately. First, we tested  
312 the impact of loss-of-function (LoF) of each homolog on trait variation with the following model:

313

$$Y \sim LoF + \varepsilon$$

314 Where Y stands for average trait values, LoF denotes the binary scores that predict potential  
315 functional loss of the homolog, and  $\varepsilon$  is the residual.

316

317 Similarly, an association model was applied to test for the impact expression/dosage changes on  
318 trait evolution:

319

$$Y \sim Expr + \varepsilon$$

320 Where  $Y$  is the trait vector,  $Expr$  stands for the expression of each homolog in  $\log_2$ -scale and  $\varepsilon$  is  
321 the residual.

322

323 A matrix of shared branch length among species in the species tree was included in the models as  
324 a random effect to control for species relatedness (shared macroevolutionary history) as proposed  
325 previously (Lynch, 1991). However, potentially due to the star-like phylogeny of the assayed  
326 species or the phylogenetically independent evolution of rhizosphere N dynamics, including this  
327 random effect term had little impact on the test results (Supplementary Figure S2). Hence, we  
328 focus on the results of the fixed effect model for simplicity.

329

### 330 **Candidate genes**

331 The moderate sample size ( $N = 36$ ) compromised the power of the above trait-by-homolog  
332 association models at a genome wide scale. Hence, we focused on an *a priori* set of 188 candidate  
333 genes previously shown to affect BNI compound synthesis and transport as well as N uptake and  
334 mobilization in maize and sorghum (Supplementary Table S4) (Léran *et al.*, 2014; Tesfamariam  
335 *et al.*, 2014; Widhalm & Rhodes, 2016; Wang *et al.*, 2020; Pan *et al.*, 2021; Otaka *et al.*, 2022;  
336 Petrolí *et al.*, 2023).

## 337 Results

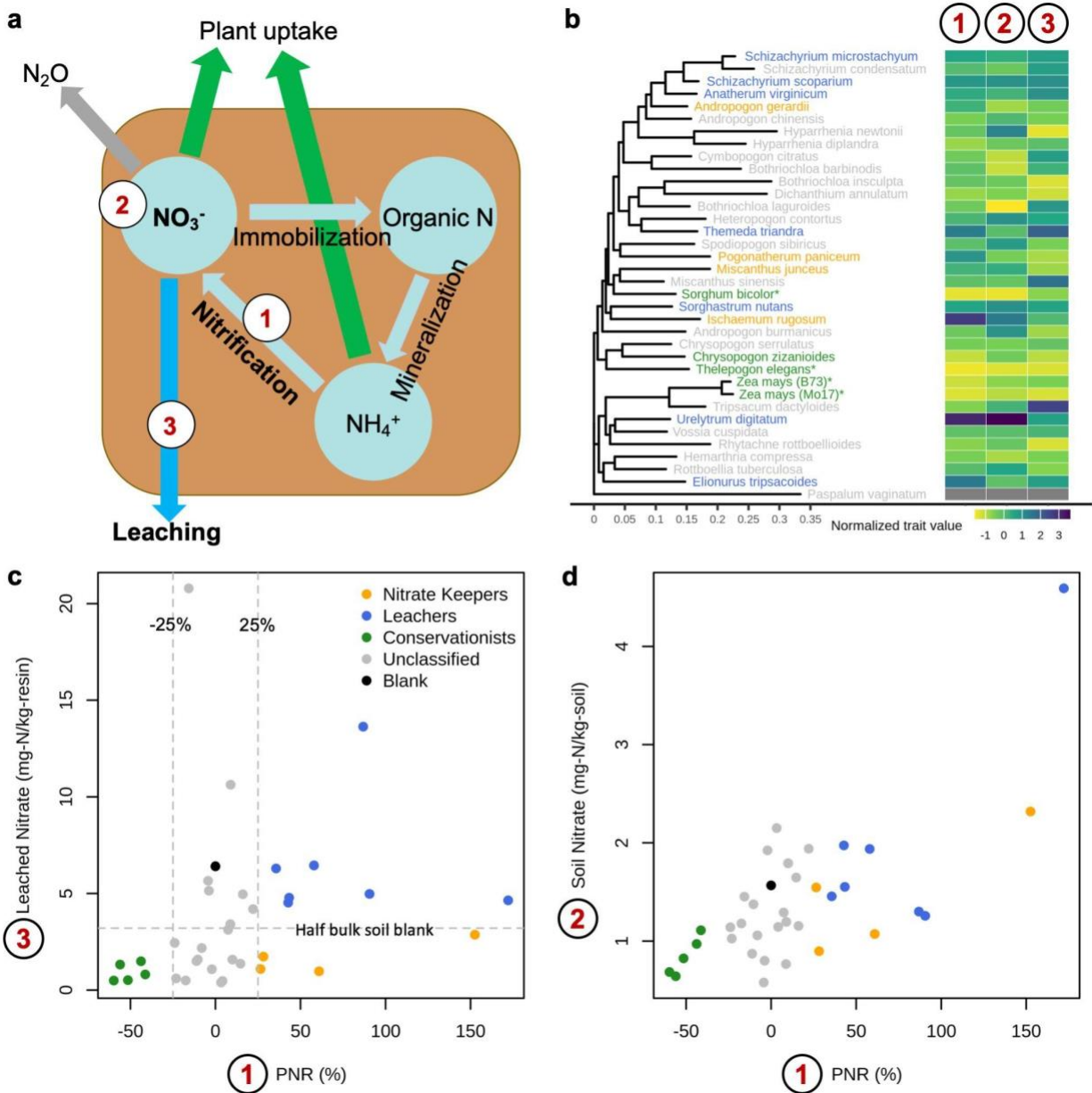
### 338 The evolution of distinct rhizosphere N cycle management strategies

339 We measured the potential nitrification rate (PNR),  $\text{NO}_3^-$  production and loss in the rhizosphere  
340 system of various Andropogoneae species grown on US corn belt soil during their active vegetative  
341 growth stage (Figure 2a). Significant variations were observed across species in all three  
342 rhizosphere N traits (Table 1). However, this variation did not show a clear association with the  
343 neutral phylogeny, indicating independent trait evolution (Figure 2b). A rhizosphere system with  
344 higher nitrification potential accumulates more  $\text{NO}_3^-$  (Figure 2d) while this does not necessarily  
345 translate to higher  $\text{NO}_3^-$  leaching (Figure 2c). This suggests that some species may be able to retain  
346 or utilize  $\text{NO}_3^-$  differently. Comparing the potential nitrification rate against the  $\text{NO}_3^-$  loss (Figure  
347 2c), we showcase that three distinct N cycle management strategies within the rhizosphere systems  
348 have evolved in the Andropogoneae tribe. Interestingly, the rhizosphere soil of all examined annual  
349 species, irrespective of domestication status (*Sorghum bicolor*, *Zea mays*, and *Thelepogon*  
350 *elegans*), exhibited pronounced nitrification inhibition (potential nitrification was reduced by 25%  
351 or more compared to bulk soil potential). These species produced and lost the least  $\text{NO}_3^-$ , thereby  
352 conserving N within the system (Figure 2c). Vetiver, *Chrysopogon zizanioides*, is the only  
353 perennial species that demonstrated similar N conservation traits. We categorize these species as  
354 “**Conservationists.**” In contrast, most perennial grasses exhibited no significant control over the  
355 nitrification rate in their rhizosphere, with some even *enhancing* nitrification markedly  
356 (nitrification was elevated by 25% or more compared to bulk soil potential). Seven of these  
357 nitrification-enhancing species (*Elionorus tripsacoides*, *Themeda triandra*, *Urelytrum digitatum*,  
358 *Sorghastrum nutans*, *Schizachyrium scoparium*, *Anatherum virginicum* and *Schizachyrium*  
359 *microstachyum*) displayed increased  $\text{NO}_3^-$  production and leaching (>50% of bulk soil  $\text{NO}_3^-$  loss),  
360 as anticipated (Figure 2c). These species are referred to as “**Leachers.**” Intriguingly, another group  
361 of species (*Ischaemum rugosum*, *Miscanthus junceus*, *Pogonatherum paniceum* and *Andropogon*  
362 *gerardi*) enhanced rhizosphere nitrification while minimizing  $\text{NO}_3^-$  loss from the system (<50%  
363 of bulk soil  $\text{NO}_3^-$  loss) (Figure 2c). We term these species “**Nitrate Keepers.**”

	median	mean	Std. deviation	C.V.	$\eta^2_{\text{taxa}}$
PNR	1.80	1.92	1.02	0.53	0.82***
Soil $\text{NO}_3^-$	1.20	1.35	0.87	0.65	0.61***
Leached $\text{NO}_3^-$	1.05	3.60	6.21	1.73	0.40'

364

365 **Table 1. Descriptive statistics for soil N measurements.** Potential nitrification rate (PNR) in  $\text{mg N kg}^{-1} \text{ hr}^{-1}$ , soil  
 366  $\text{NO}_3^-$  concentration ( $\text{mg N kg}^{-1}$ ; PPM) and leached  $\text{NO}_3^-$  concentration ( $\text{mg N kg}^{-1}$ ; PPM). The sample size equals 112  
 367 which is composed of 37 taxa each with 1-3 replicates. The variance explained by taxa ( $\eta^2_{\text{taxa}}$ ) are calculated based on  
 368 the analysis of variance (ANOVA) using log-transformed trait data as following:  $\eta^2_{\text{taxa}} = \text{SS}_{\text{taxa}}/\text{SS}_{\text{total}}$ . The significance  
 369 of the taxa term in ANOVA is denoted as following: \*\*\*  $p < 0.001$ ; \*  $p < 0.1$ .  
 370  
 371



372

373 **Figure 2. Soil N measurements and the classification of distinct rhizosphere N managing strategies.**

374 **a.** Illustration of the soil N cycle. Soil N exists as organic N,  $\text{NH}_4^+$  and  $\text{NO}_3^-$ . Via mineralization processes, organic N  
375 is mobilized into  $\text{NH}_4^+$ .  $\text{NH}_4^+$  can be nitrified into  $\text{NO}_3^-$ . Through immobilization processes, inorganic  $\text{NO}_3^-$  turns back  
376 into organic N. Due to high mobility,  $\text{NO}_3^-$  is more likely to escape the system, either through leaching or subjected  
377 to denitrification and turned to  $\text{N}_2$  and  $\text{N}_2\text{O}$ . Given our focus on how diverse grass species manage their rhizosphere  
378 N budget, we measured (1) the potential nitrification rates (PNR) in different studied taxa relative to a bulk soil blank  
379 sample (in percentage), (2) soil nitrate concentrations (PPM) and (3) the amount of nitrate leached (PPM). **b.**  
380 Phylogenetically independent evolution of the rhizosphere N traits. Extremes of the measured rhizosphere N traits  
381 evolved multiple times across the Andropogoneae phylogeny. Trait values are shown after normalization ( $(x-$   
382  $\text{mean}(x))/\text{sd}(x)$ ) as heatmap. Colors in tip labels refer to panel c. **c-d.** Scatter plots amongst the three measured N traits.  
383 The classification of distinct rhizosphere N managing strategies for different taxa is based on c. Relative to a bulk soil  
384 blank sample, “Conservationists” inhibit PNR by 25% or more and leach  $\text{NO}_3^-$  by 50% or less; “Leachers” elevated  
385 PNR by 25% or more and leach  $\text{NO}_3^-$  by 50% or more, and “Nitrate keepers” increase PNR by 50% or more but lost  
386  $\text{NO}_3^-$  by 50% or less.

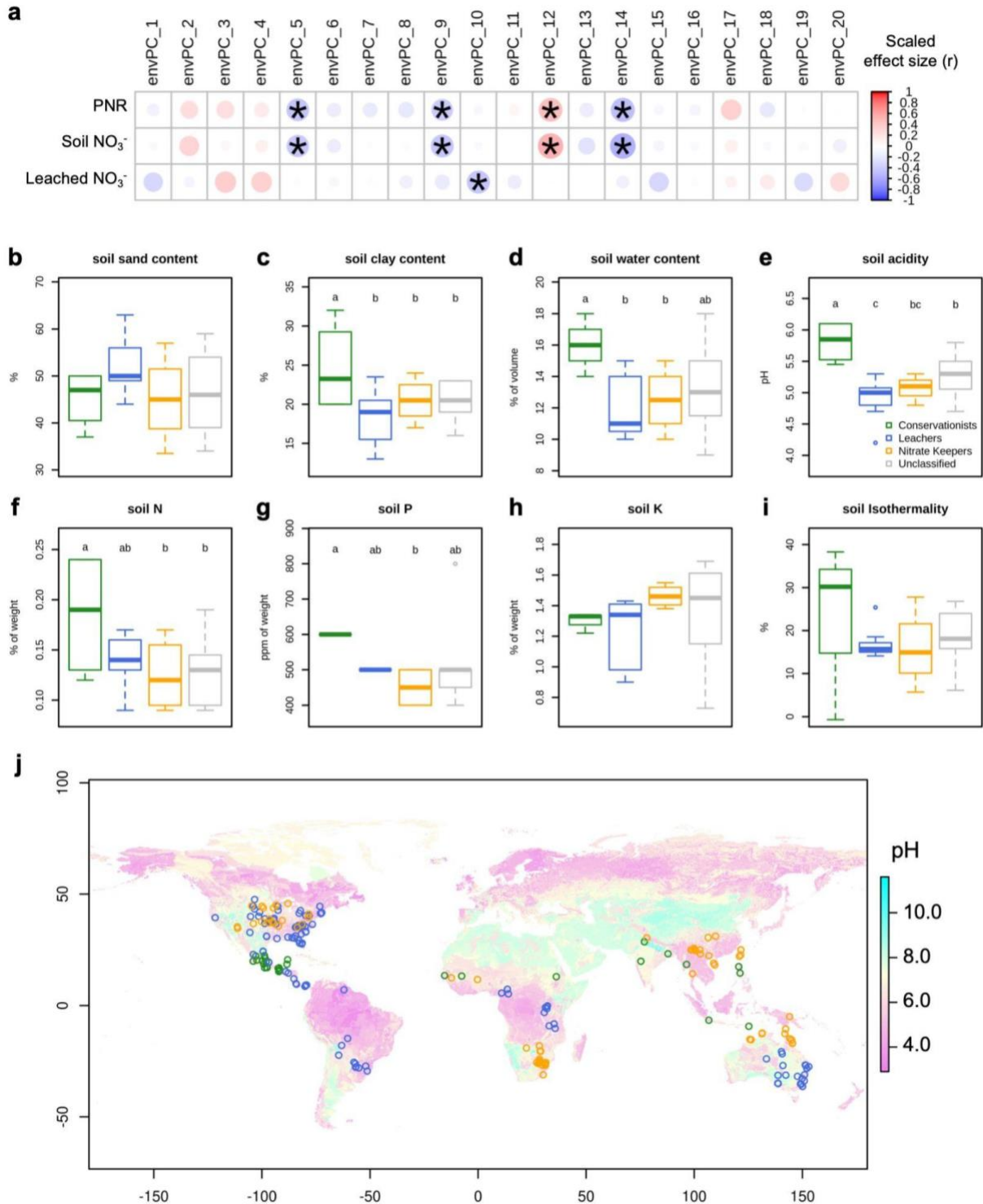
387

### 388 **Ecological selection on rhizosphere N cycle**

389 To understand the potential ecological selection forces that drive the evolution of distinct  
390 rhizosphere N management strategies in different species, we associated the biogeography and  
391 habitat environmental conditions of diverse Andropogoneae species with their rhizosphere N traits.  
392 The range records of different species were retrieved from the Botanical Information and Ecology  
393 Network (BIEN). Using all the documented occurrence coordinates, we collected a total of 291  
394 environmental features (see materials and methods) and summarized the environmental variation  
395 with 20 principal components (envPCs) which account for >80% of the total environmental  
396 variance (Supplementary Figure S3). Association analysis revealed five envPCs that significantly  
397 explain the rhizosphere N trait variation (Figure 3a). Several soil characteristics (e.g. acidity,  
398 nutrient composition, temperature, particle size...etc) and climatic factors (e.g. isothermality)  
399 loaded heavily on the significant rhizosphere N-associated envPCs (Supplementary Figure S4).  
400 “Leachers” originate from areas with drier and sandier soil with high leaching potential (Figure  
401 3b-d). “Conservationists” with nitrification inhibitory effects are adapted to less acidic (Figure 3e  
402 and j), more fertile (Figure 3f and g) soil where nitrifying microbes may be more active. We also  
403 observed slightly higher soil isothermality (i.e. diurnal changes are closer to seasonal difference)  
404 in the habitat range of the “Conservationists” (Figure 3i). The “Nitrate keepers” originally live on  
405 potassium (K)-rich soil (Figure 3h). This result implied that the diverse rhizosphere N management

406 strategies in the Andropogoneae tribe may evolve as potential adaptive responses in distinct  
 407 ecological niches.

408



409

410 **Figure 3. The association of rhizosphere N traits and the native habitat environments.**

411 **a.** A summary of the association analyses between the habitat environments of different species and their rhizosphere  
412 N traits. The habitat environments of different species are summarized with a principal component analysis (PCA) of  
413 282 environmental features, where the top 20 envPCs explained >80% of total variance. A list of the environmental  
414 features and the loading of the PCA is available in Supplementary table S2. We test the association of each envPC  
415 with each rhizosphere N trait. Each cell indicates an independent test. The color and the circle size denote the effect  
416 of the association (Pearson's correlation coefficient). Asterisks denote statistical significance ( $p < 0.05$ ). Five envPCs  
417 significantly co-vary with the rhizosphere N trait variation. We select a subset of the top contributing environmental  
418 features to these significant envPCs and visualize the difference between species with different rhizosphere N  
419 managing strategies. These include **b.** soil sand content, **c.** soil clay content, **d.** soil water content, **e.** soil pH, **f.** soil N,  
420 **g.** soil phosphate (P), **h.** soil potassium (K) and **i.** soil isothermality. Small case letters denote statistical grouping  
421 based on Fisher's Least Significant Difference test. **j.** A map of global soil acidity (pH) with species occurrence records  
422 (empty dots) overlaid. Occurrence data are retrieved for each studied Andropogoneae species from the BIEN database.  
423 Species with >20 occurrence records are down-sampled to 20 records for visual clarity. Dot colors follow the species  
424 group colors denoted in panel e. Both leacher and nitrate keeper species (blue and orange) showed occurrence in more  
425 acidic environments.

426

427 **Genetic basis of the variation in rhizosphere N cycle**

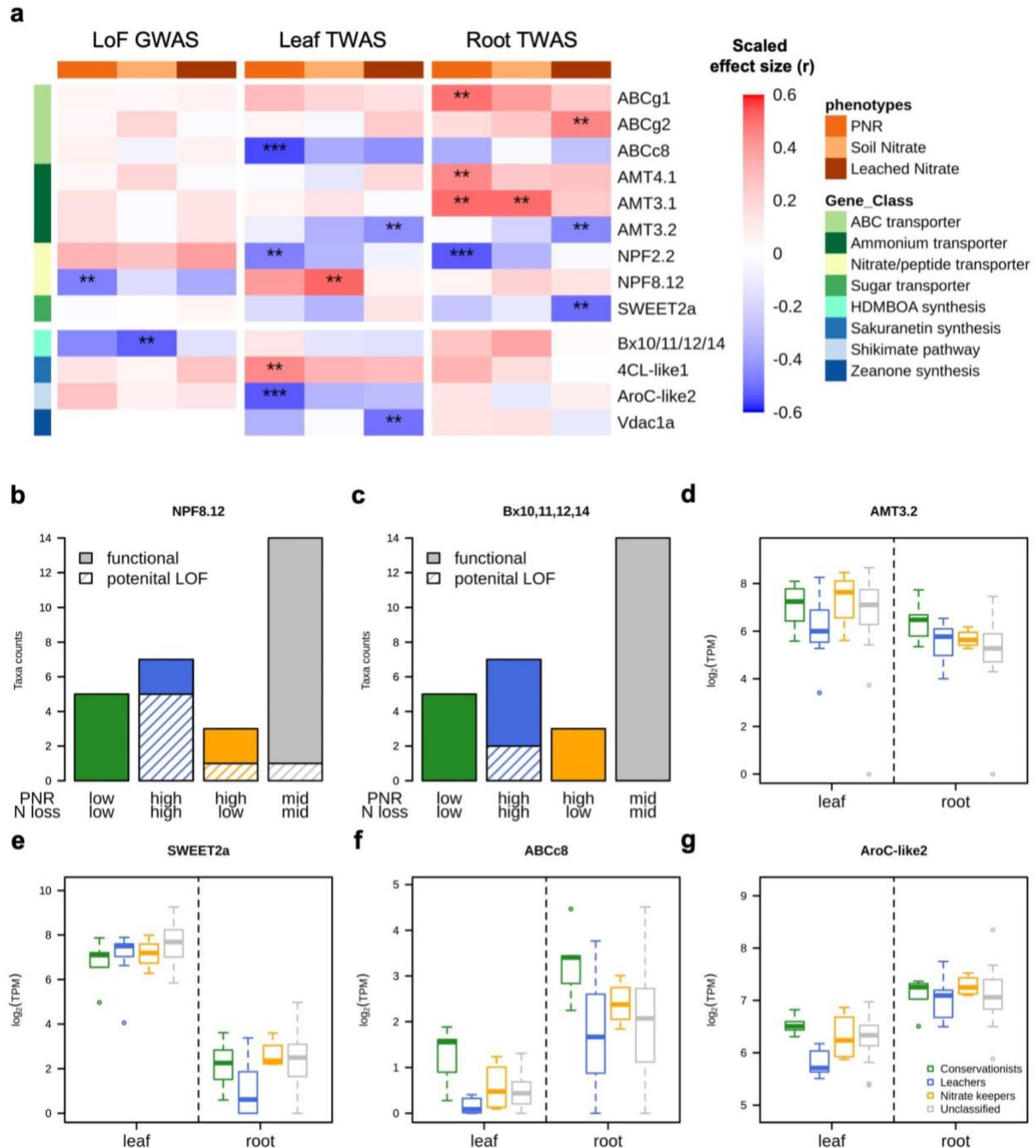
428 Next, we explored how the potential loss of function and regulatory evolution of the homologs  
429 affect the rhizosphere N cycle. With a linear modeling framework, we conducted a total of nine  
430 sets of cross-species association analyses between the three rhizosphere N traits (PNR, soil  $\text{NO}_3^-$   
431 and  $\text{NO}_3^-$  loss) and three genetic factors (loss of function prediction, leaf expression and root  
432 expression). The moderate number of species assayed in this study limits the statistical power of  
433 the association models. Therefore, we focus our gene discovery on a set of 188 candidates  
434 (Supplementary Table S4) identified from previous works (Léran *et al.*, 2014; Tesfamariam *et al.*,  
435 2014; Widhalm & Rhodes, 2016; Wang *et al.*, 2020; Pan *et al.*, 2021; Otaka *et al.*, 2022; Petroli *et*  
436 *al.*, 2023). We aim to test for shared evolution signatures in multiple species that evolved similar  
437 rhizosphere N managing strategies. Compared to a random set of homologs, *a priori* candidate  
438 homologs are enriched for significant association at the p-value threshold of 0.01, particularly  
439 between root expression profiles and rhizosphere N traits (Supplementary Figure S5). We  
440 identified 13 homologs that are key to the variation of rhizosphere N cycle in diverse species  
441 (Figure 4a and Supplementary Figure S6; Supplementary Table S5).

442

443 The significant candidates mostly encode transporter proteins, which include three ammonium  
444 transporters (AMTs), two nitrate/peptide transporter family proteins (NPFs), one sugar  
445 transporters (SWEETs) and three ABC-type transporters (Figure 4a). The potential loss of function  
446 of ZmNPF8.12 homolog is significantly associated with higher nitrification rate. >70% of the  
447 Leachers, which produced and lost the most  $\text{NO}_3^-$ , do not have a functional copy of this homolog  
448 (Figure 4b). In line with this, we detected a signature of relatively constrained evolution for  
449 ZmNPF8.12 homologs in the Conservationists species (codeml-branch model; likelihood ratio =  
450 6.58,  $p = 0.01$ ). Leaf expression of the ZmNPF2.2/2.3 homolog appears to be important for N  
451 conservation (Supplementary Figure S7). The homolog of ZmAMT3.2 exhibits relatively high  
452 expression in the roots of the Conservationists species which exhibit strong nitrification inhibitory  
453 effects (Figure 4d). Root expression of the ZmSWEET2a homolog is associated with lower  $\text{NO}_3^-$   
454 leaching, with low expression in the roots of the leacher species (Figure 4e). In addition to the  
455 nutrient transporters, the expression of the ZmABCc8 homolog is negatively correlated with  
456 rhizosphere nitrification rate (Figure 4f).

457  
458 Four homologs of the genes involved in BNI metabolite biosynthesis were detected, one of which  
459 is found in the benzoxazinoid biosynthetic pathway (Figure 4a). HDMBOA, an important BNI  
460 metabolite in maize (Otaka *et al.*, 2022), is a benzoxazinoid derivative (2-hydroxy-4,7-dimethoxy-  
461 1,4-benzoxazin-3-one). Potential loss of function of the ZmBx10/11/12/14 homolog, which  
462 catalyzes the synthesis of the storage form HDMBOA-glucoside (Otaka *et al.*, 2022), is associated  
463 with increased production of rhizosphere  $\text{NO}_3^-$  (Figure 4a): we only observe putative loss of  
464 function events in two Leacher species (Figure 4c). In addition, we also observe a significant  
465 negative correlation between the  $\text{NO}_3^-$  loss rate and the leaf expression of ZmVdac1a homolog.  
466 ZmVdac1a encodes an isochorismate synthase which is potentially important for the synthesis of  
467 zeaxone, another BNI metabolite in maize (Otaka *et al.*, 2022). The leaf expression of another  
468 homolog encoding a ZmAroC-like protein correlates negatively with soil nitrification: higher  
469 expression is observed in the conservationist species (Figure 4g).

470



471

472 **Figure 4. Genes underlying the rhizosphere N trait variation.**

473 **a.** A summary of the significant association between different genetic factors (i.e. LoF prediction and expression  
 474 estimates) and the rhizosphere N traits across species for the candidate homologs. For each homolog, there are nine  
 475 association tests (three genetic factors by three rhizosphere N traits) as denoted by the columns. Each row is a homolog  
 476 that exhibits significant association in at least one trait-genetic combination. Row annotation colors indicate the gene  
 477 classes each significant homolog belongs to. The cell colors denote the strength and direction of the association

478 (Pearson's correlation coefficient,  $r$ ). Stars denote statistical significance (\*\*:  $p < 0.01$ ; \*\*\*:  $p < 0.001$ ). The same test  
479 summary for all tested homologs is available as Supplementary Figure S6. **b. & c.** Bar plots demonstrating the  
480 occurrence of potential LoF in different species groups with distinct rhizosphere N traits for the homologs of NPF8.12  
481 and Bx10,11,12,14 respectively. Bar heights indicate the count of taxa. Colors denote the species groups. Solid bars  
482 represent the functional copies while slashed bars indicate potential loss of function. **d-g.** Homolog expression profiles  
483 in different tissues (left: leaf and right: root) in different species groups with distinct rhizosphere N traits (colors) for  
484 a subset of candidates: **d.** AMT3.2, **e.** SWEET2a, **f.** ABCc8, and **g.** AroC-like2. The remaining significant homolog-  
485 trait associations are visualized in Supplementary Figure S7.

486

487 Despite the limited statistical power, top outliers with the strongest association signatures among  
488 all tested homologs may also be reliable candidates, in addition to the *a priori* ones. We identified  
489 the top five candidates in each of the nine association tests and collected a union set of 40 homologs  
490 (Supplementary Table S5). These homologs are enriched for biological functions related to defense  
491 responses (GO:0050832, GO:0042742 and GO:0031640) as well as cell wall and polysaccharide  
492 catabolic processes (GO:0006032, GO:0016998 and GO:0000272) (Supplementary Table S6).  
493 The potential loss of function in a homolog encoding a knottin scorpion toxin-like protein and low  
494 root expression of the ZmSod2 (superoxide dismutase) homolog are linked to elevated  $\text{NO}_3^-$  loss.  
495 Additionally, increased expression of several homologs with putative chitinase, cellulase, and  
496 laccase activities correlates with higher  $\text{NO}_3^-$  loss. These findings highlight the significance of  
497 plant-microbe interactions in the rhizosphere for soil N dynamics.

498

## 499 Discussion

500 In this study, we present the first systematic screening for rhizosphere N dynamics in dozens of  
501 grass species with wide adaptive ranges, identifying three distinct patterns of N-cycling (Figure  
502 5). BNI capacity, in combination with a “more ammonium” management, was proposed as one  
503 important trait for soil N sustainability (Subbarao & Searchinger, 2021). The documentation and  
504 success of BNI capacities in perennial grasses in tropical savannas (Subbarao *et al.*, 2007a;  
505 Srikanthasamy *et al.*, 2018) and pasture systems (Baruch *et al.*, 1985; Rossiter-Rachor *et al.*, 2009)  
506 gave rise to the hypothesis that some Andropogoneae species may present enhanced BNI capacity  
507 and potentially favorable rhizosphere N traits that are not observed in the standing genetic variation  
508 of domesticated annual maize. However, we observe little evidence supporting this hypothesis.  
509 Despite substantial variation across diverse Andropogoneae species, only one wild annual grass,  
510 *Thelepogon elegans*, exhibits slightly higher BNI capacity and N conservation than the  
511 domesticated annuals in our experiment. Both annual crops assayed in this experiment, maize and  
512 sorghum, are already good N Conservationists. This result undermines the leverage of tribe-level  
513 phylogenetic diversity for BNI improvement in maize. However, the systematic assays of diverse  
514 grasses allowed unprecedented biogeographic and cross-species genomic/transcriptomic analyses  
515 on the emergence and evolution of rhizosphere N cycles (Figure 5).

516  
517 Three out of the four conservationist species exhibit annual life history, implicating potential  
518 benefit of such N conservation traits during the perennial-annual transition. We observed that the  
519 conservationist species originate from more fertile areas (high N and P; Figure 3f-g and Figure 5).  
520 In contrast to the hypothesis that low N availability drives the evolution of BNI (Lata *et al.*, 2022),  
521 our result suggests the competition with nitrifiers for more available N may be the driving force  
522 for the emergence of BNI. Notably, in addition to N fertility, we also observed a significant  
523 association between BNI capacity and soil pH. Species with high BNI capacity grow on less acidic  
524 soil (Figure 3e and Figure 5). Independent evidence for the emergence of BNI capacity during the  
525 adaptation to alkali soils was also documented recently (Wang *et al.*, 2023; Przybylska *et al.*,  
526 2024). We expect limited nitrifier populations in more acidic environments as the nitrification  
527 reaction is largely inhibited when soil pH is below 5 (Dancer *et al.*, 1973). Hence, we hypothesize  
528 that BNI capacity and NH<sub>4</sub><sup>+</sup> conservation mechanisms in a few Andropogoneae grasses could  
529 emerge in competition with nitrifying bacteria during evolution. Nevertheless, maize field soil was

530 used in our common garden experiment so it is also possible that the lack of nitrification inhibitory  
531 or even stimulating effects in some of the wild species may be mal-adaptive plasticity in response  
532 to the foreign soil and microbes. Multiple common garden experiments including distinct soil types  
533 or reciprocal transplantation between some species pairs will provide further insights into this  
534 hypothesis.

535

536 The discovery of Nitrate Keepers, which enhanced nitrification while conserving  $\text{NO}_3^-$ , is  
537 interesting. There is massive variation in the preference between  $\text{NH}_4^+$  and  $\text{NO}_3^-$  among plant  
538 species (Houlton *et al.*, 2007; Kahmen *et al.*, 2008; Boudsocq *et al.*, 2012; Britto & Kronzucker,  
539 2013), and such preference determines the fitness benefits and cost of BNI capacity (Boudsocq *et*  
540 *al.*, 2012; Konaré *et al.*, 2019). Stimulation of nitrification can be particularly beneficial for  $\text{NO}_3^-$   
541 -preferring species in competition to  $\text{NH}_4^+$ -preferring plants. The example of two ecotypes with  
542 opposing effects on nitrification for *Hyparrhenia diplandra* (Lata *et al.*, 2000) highlights the  
543 presence of environment-specific plant-plant and plant-microbe competition for different N-  
544 sources and the evolution of locally adapted soil N management strategies. Therefore, we speculate  
545 the “Nitrate Keepers” may exhibit a preferential uptake of  $\text{NO}_3^-$  over  $\text{NH}_4^+$  while further  
546 experiments are still needed.

547

548 In this study, each species was represented by only one genotype, which is a potential caveat:  
549 different ecotypes within a species might influence soil chemistry differently (e.g. (Lata *et al.*,  
550 2000). Examining within-species variation, while potentially important and insightful, was beyond  
551 the scope of the study, which was designed for broad interspecific differences exploration. We  
552 encourage future studies to follow up on the variation within a couple of the species or to include  
553 multiple genotypes per species in similar analyses.

554

555 This substantial cross-species variation in rhizosphere N dynamics underscores the importance of  
556 understanding the genetic underpinnings of these traits. The enrichment of transporter-encoding  
557 homologs, particularly N transporters, in our cross-species association analyses consistently  
558 highlights the relevance of soil N dynamics and plant preference. On the one hand, nitrification-  
559 inhibiting Conservationists have higher root expression of ammonium transporter (ZmAMT3.2),  
560 implicating their potential preference for conserved  $\text{NH}_4^+$  (Figure 4d and Figure 5). On the other

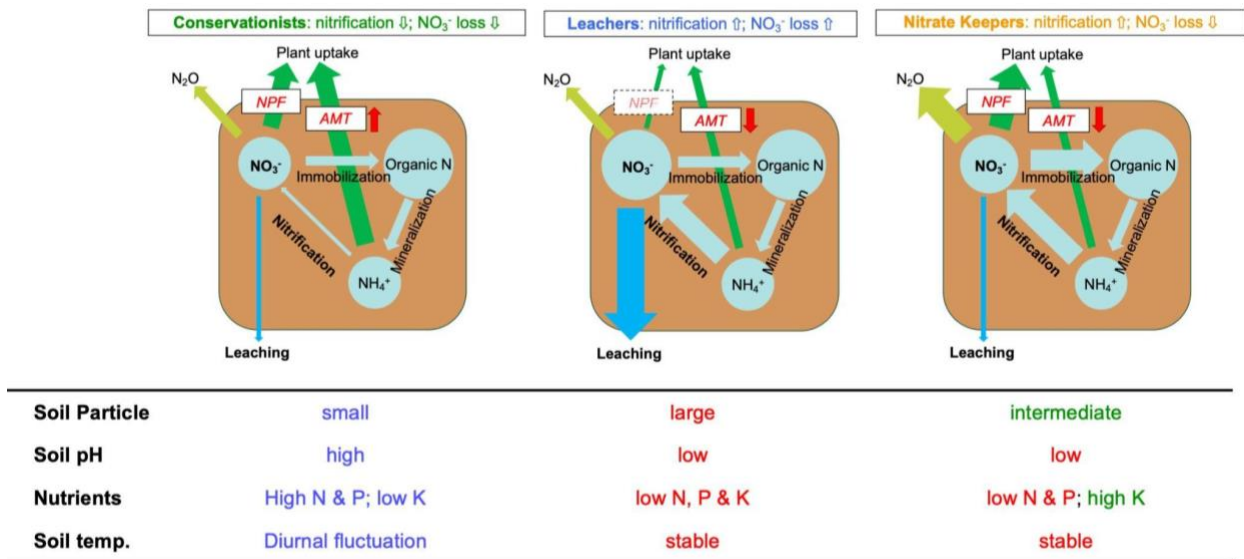
561 hand, most Nitrate Keepers exhibit lower root expression of ZmAMT3.2 (Figure 4d) but preserve  
562 a functional copy of the ZmNPF8.12 nitrate transporter homolog unlike the Leachers, implying  
563 their potential preference for NO<sub>3</sub><sup>-</sup> (Figure 4b and Figure 5) Interestingly, another ammonium  
564 transporter paralog, ZmAMT5, was identified in a recent GWAS study on maize BNI (Petroli *et*  
565 *al.*, 2023). The independent discovery of association between BNI activity and AMT gene family  
566 supports the interaction between N uptake/preference and soil nitrification modification.

567  
568 Besides N transporters, several homologs encoding ABC-type transporters were identified by our  
569 association analyses. A homolog of ABC type c transporter (ZmABCc8) showed higher expression  
570 in the nitrification-inhibiting Conservationist species. Maize ZmABCc8 and its ortholog in  
571 Arabidopsis were reported to be involved in the transport of anthocyanin (Goodman *et al.*, 2004;  
572 Dean *et al.*, 2022). Anthocyanin and other flavonoids play a role in copper chelation (Sarma *et al.*,  
573 1997), which is thought to be one nitrification inhibitory mechanism (Corrochano-Monsalve *et al.*,  
574 2021). Therefore, we hypothesized that the identified ABC type c transporter may be responsible  
575 for the exudation of BNI compounds and thus their expression correlates with the BNI capacity.

576  
577 In addition to the transporters, we also detected significant association in a handful of homologs  
578 involved in the biosynthesis of known BNI compounds in maize and sorghum. The identification  
579 of homologs involved in the biosynthesis and the modification of chorismate highlight its central  
580 role in the synthesis of BNI metabolites. However, the wide variety of BNI compounds found in  
581 different BNI-species (Subbarao *et al.*, 2007b, 2013; Pariasca Tanaka *et al.*, 2010; Sun *et al.*, 2016;  
582 Otaka *et al.*, 2022) suggests the presence of multiple biochemical routes for the gain of BNI  
583 capacity. This poses a challenge for the identification of more genes with convergent  
584 functional/regulatory evolution.

585  
586 The choice of US corn belt soil for the experiment makes our results directly relevant to modern  
587 maize production. Our systematic exploration of phylogenetic diversity in rhizosphere N dynamics  
588 offers insights into how and/or to which extent breeding efforts could reduce the environmental  
589 impact of maize agriculture. Fine-tuning the regulation of our candidate transporters may help  
590 optimize maize rhizosphere N balance. For instance, early expression of AMTs might make maize  
591 better fit to the “more-ammonium” management (Subbarao & Searchinger, 2021). The discovery

592 of  $\text{NO}_3^-$  keeping strategies also highlight the potential of early and efficient nitrate uptake. Since  
 593 maize evolved as one of the conservationists in the tribe, favorable alleles might have emerged  
 594 and segregated as natural variation within maize. The field will need more studies like the recent  
 595 GWAS (Petroli *et al.*, 2023) to tap the genetic diversity within maize and more exploration in other  
 596 wild annual *Zea* species not included in this study. Beyond genetic improvement for N uptake and  
 597 conservation during the growing season of the annual crops, the integration of cover crops and  
 598 intercropping into the agricultural system can also be crucial, if not more so, for mitigating early  
 599 spring nitrogen loss (Parkin *et al.*, 2016; Zhang *et al.*, 2023; Rogovska *et al.*, 2023).  
 600



601  
 602 **Figure 5. Schematic illustration of diverse rhizosphere N cycles in Andropogoneae.**  
 603 This figure illustrates the hypothetical rhizosphere N cycles of three species groups with distinct  
 604 rhizosphere N managing strategies evolved in the Andropogoneae tribe: Conservationists, Leachers, and  
 605 Nitrate Keepers. The Conservationists inhibit nitrification and potentially uptake the conserved  $\text{NH}_4^+$  with  
 606 the higher expression of ZmAMT3.2 homolog. The Leachers stimulate nitrification but are not able to  
 607 utilize the converted  $\text{NO}_3^-$  potentially due to the lack of functional ZmNPF8.12 nitrate transporter. In  
 608 contrast, the Nitrate Keepers possess functional copies of ZmNPF8.12 and thus they lose less  $\text{NO}_3^-$ .  
 609 Conservationists originate from more fertile, less acidic and moist soils. In contrast, the Leachers are from  
 610 habitats with drainage and/or nutrient stresses. One key difference between the habitats of the Nitrate  
 611 Keepers and the one of the Leachers is the drainage stress.  
 612

613 **Acknowledgement**

614 This project is supported by the NSF PanAnd Grant Award #1822330 and USDA-ARS. Thank  
615 you Corteva and INARI for genomic data generation. Thank you Sara Miller, Zong-Yan Liu, Sam  
616 Herr and Elad Oren for support on sample collection during the experiment. Graph design is  
617 facilitated by resources on Flaticon.com, D-ALLE, and BioRender.com.

618

619 **Conflict of interest**

620 The authors declare no conflict of interest.

621

622 **Author contribution**

623 S-KH, BDE, SSR, ADK, CR, and ESB designed the research. TMA-E and EAK collected the  
624 materials of the research. S-KH, NL, TL, BDE and AJH performed the experiment and collected  
625 the data. S-KH, BDE, GC-N, AJS and COH analyzed the data. S-KH, BDE, GC-N, SSR, JOO-R,  
626 EAK and ESB were involved in result interpretations. S-KH drafted the manuscript and all other  
627 authors edited the manuscript.

628

629 **Data availability**

630 All data, source scripts, analytical notebooks and intermediate outputs are available at  
631 ([https://bitbucket.org/bucklerlab/p\\_evolution/publication/src/main/](https://bitbucket.org/bucklerlab/p_evolution/publication/src/main/)). The raw sequencing read  
632 data in this study have been submitted to the NCBI BioProject database  
633 (<https://www.ncbi.nlm.nih.gov/bioproject/>) under accession number PRJEB50280 (genomic long  
634 read), PRJNA543119 (genomic short reads) and PRJNA1119410 (RNA short reads). Short read  
635 assemblies will be made available on Zenodo upon publication (10.5281/zenodo.1122298).

636

637 **Reference**

638 **Abalos D, van Groenigen JW, De Deyn GB. 2018.** What plant functional traits can reduce  
639 nitrous oxide emissions from intensively managed grasslands? *Global change biology* **24**: e248–  
640 e258.

641 **Bachle S, Zaricor M, Griffith D, Qui F, Still CJ, Ungerer MC, Nippert JB. 2022.**  
642 Physiological responses to drought stress and recovery reflect differences in leaf function and  
643 anatomy among grass lineages. *bioRxiv*: 2022.07.30.502130.

644 **Baruch Z, Ludlow MM, Davis R. 1985.** Photosynthetic responses of native and introduced C4  
645 grasses from Venezuelan savannas. *Oecologia* **67**: 388–393.

646 **Bender RR, Haegele JW, Ruffo ML, Below FE. 2013.** Nutrient uptake, partitioning, and  
647 remobilization in modern, transgenic insect-protected maize hybrids. *Agronomy journal* **105**:  
648 161–170.

649 **Billen G, Garnier J, Lassaletta L. 2013.** The nitrogen cascade from agricultural soils to the sea:  
650 modelling nitrogen transfers at regional watershed and global scales. *Philosophical transactions*  
651 *of the Royal Society of London. Series B, Biological sciences* **368**: 20130123.

652 **Boudsocq S, Niboyet A, Lata JC, Raynaud X, Loeuille N, Mathieu J, Blouin M, Abbadie L,**  
653 **Barot S. 2012.** Plant preference for ammonium versus nitrate: a neglected determinant of  
654 ecosystem functioning? *The American naturalist* **180**: 60–69.

655 **Bremner JM, Blackmer AM. 1978.** Nitrous oxide: emission from soils during nitrification of  
656 fertilizer nitrogen. *Science* **199**: 295–296.

657 **Britto DT, Kronzucker HJ. 2013.** Ecological significance and complexity of N-source  
658 preference in plants. *Annals of botany* **112**: 957–963.

659 **Byrnes RC, Nùñez J, Arenas L, Rao I, Trujillo C, Alvarez C, Arango J, Rasche F, Chirinda**  
660 **N. 2017.** Biological nitrification inhibition by *Brachiaria* grasses mitigates soil nitrous oxide  
661 emissions from bovine urine patches. *Soil biology & biochemistry* **107**: 156–163.

662 **Corrochano-Monsalve M, González-Murua C, Bozal-Leorri A, Lezama L, Artetxe B. 2021.**

- 663 Mechanism of action of nitrification inhibitors based on dimethylpyrazole: A matter of chelation.  
664 *The Science of the total environment* **752**: 141885.
- 665 **Cowan MF, Blomstedt CK, Norton SL, Henry RJ, Møller BL, Gleadow R. 2020.** Crop wild  
666 relatives as a genetic resource for generating low-cyanide, drought-tolerant Sorghum.  
667 *Environmental and experimental botany* **169**: 103884.
- 668 **Dancer WS, Peterson LA, Chesters G. 1973.** Ammonification and nitrification of N as  
669 influenced by soil pH and previous N treatments. *Soil Science Society of America journal. Soil*  
670 *Science Society of America* **37**: 67–69.
- 671 **Dean JV, Willis M, Shaban L. 2022.** Transport of acylated anthocyanins by the Arabidopsis  
672 ATP-binding cassette transporters AtABCC1, AtABCC2, and AtABCC14. *Physiologia*  
673 *plantarum* **174**: e13780.
- 674 **Doane TA, Horwath WR. 2003.** Spectrophotometric Determination of Nitrate with a Single  
675 Reagent. *Analytical letters* **36**: 2713–2722.
- 676 **EPA. 2023.** *Inventory of U.S. Greenhouse Gas Emissions and Sinks: 1990-2021.*
- 677 **Esteban R, Ariz I, Cruz C, Moran JF. 2016.** Review: Mechanisms of ammonium toxicity and  
678 the quest for tolerance. *Plant science: an international journal of experimental plant biology*  
679 **248**: 92–101.
- 680 **Estep MC, McKain MR, Vela Diaz D, Zhong J, Hodge JG, Hodkinson TR, Layton DJ,**  
681 **Malcomber ST, Pasquet R, Kellogg EA. 2014.** Allopolyploidy, diversification, and the  
682 Miocene grassland expansion. *Proceedings of the National Academy of Sciences of the United*  
683 *States of America* **111**: 15149–15154.
- 684 **Fick SE, Hijmans RJ. 2017.** WorldClim 2: new 1-km spatial resolution climate surfaces for  
685 global land areas. *International Journal of Climatology* **37**: 4302–4315.
- 686 **GAEZ v4 Data Portal.**
- 687 **Goodman CD, Casati P, Walbot V. 2004.** A multidrug resistance-associated protein involved  
688 in anthocyanin transport in *Zea mays*. *The Plant cell* **16**: 1812–1826.

- 689 **Hartman MD, Burnham M, Parton WJ, Finzi A, DeLucia EH, Yang WH. 2022.** In silico  
690 evaluation of plant nitrification suppression effects on agroecosystem nitrogen loss. *Ecosphere*  
691 **13**.
- 692 **Hart SC, Stark JM, Davidson EA, Firestone MK. 1994.** Nitrogen Mineralization,  
693 Immobilization, and Nitrification. In: SSSA Book Series. Methods of Soil Analysis. Madison,  
694 WI, USA: Soil Science Society of America, 985–1018.
- 695 **Hijmans RJ, Bivand R, Pebesma E, Sumner MD. 2023.** *terra: R package for spatial data*  
696 *handling*. Github.
- 697 **Houlton BZ, Sigman DM, Schuur EAG, Hedin LO. 2007.** A climate-driven switch in plant  
698 nitrogen acquisition within tropical forest communities. *Proceedings of the National Academy of*  
699 *Sciences of the United States of America* **104**: 8902–8906.
- 700 **Hufford MB, Seetharam AS, Woodhouse MR, Chougule KM, Ou S, Liu J, Ricci WA, Guo**  
701 **T, Olson A, Qiu Y, et al. 2021.** De novo assembly, annotation, and comparative analysis of 26  
702 diverse maize genomes. *Science* **373**: 655–662.
- 703 **Husson F, Josse J. 2023.** *missMDA — Handling Missing Values with Multivariate Data*  
704 *Analysis*. Github.
- 705 **Husson F, Josse J, Le S, Mazet J. 2023.** *FactoMineR: Package FactoMineR*. Github.
- 706 **Kahmen A, Wanek W, Buchmann N. 2008.** Foliar delta(15)N values characterize soil N  
707 cycling and reflect nitrate or ammonium preference of plants along a temperate grassland  
708 gradient. *Oecologia* **156**: 861–870.
- 709 **Katoh K, Misawa K, Kuma K-I, Miyata T. 2002.** MAFFT: a novel method for rapid multiple  
710 sequence alignment based on fast Fourier transform. *Nucleic acids research* **30**: 3059–3066.
- 711 **Khush GS. 2001.** Green revolution: the way forward. *Nature reviews. Genetics* **2**: 815–822.
- 712 **Konaré S, Boudsocq S, Gignoux J, Lata J-C, Raynaud X, Barot S. 2019.** Effects of Mineral  
713 Nitrogen Partitioning on Tree–Grass Coexistence in West African Savannas. *Ecosystems* **22**:  
714 1676–1690.

- 715 **Kosola KR, Eller MS, Dohleman FG, Olmedo-Pico L, Bernhard B, Winans E, Barten TJ,**  
716 **Brzostowski L, Murphy LR, Gu C, et al. 2023.** Short-stature and tall maize hybrids have a  
717 similar yield response to split-rate vs. pre-plant N applications, but differ in biomass and nitrogen  
718 partitioning. *Field crops research* **295**: 108880.
- 719 **Lata JC, Guillaume K, Degrange V, Abbadie L, Lensi R. 2000.** Relationships between root  
720 density of the African grass *Hyparrhenia diplandra* and nitrification at the decimetric scale: an  
721 inhibition-stimulation balance hypothesis. *Proceedings. Biological sciences / The Royal Society*  
722 **267**: 595–600.
- 723 **Lata J-C, Le Roux X, Koffi KF, Yé L, Srikanthasamy T, Konaré S, Barot S. 2022.** The  
724 causes of the selection of biological nitrification inhibition (BNI) in relation to ecosystem  
725 functioning and a research agenda to explore them. *Biology and fertility of soils* **58**: 207–224.
- 726 **Lembrechts JJ, van den Hoogen J, Aalto J, Ashcroft MB, De Frenne P, Kemppinen J,**  
727 **Kopecký M, Luoto M, Maclean IMD, Crowther TW, et al. 2022.** Global maps of soil  
728 temperature. *Global change biology* **28**: 3110–3144.
- 729 **Léran S, Varala K, Boyer J-C, Chiurazzi M, Crawford N, Daniel-Vedele F, David L,**  
730 **Dickstein R, Fernandez E, Forde B, et al. 2014.** A unified nomenclature of NITRATE  
731 TRANSPORTER 1/PEPTIDE TRANSPORTER family members in plants. *Trends in plant*  
732 *science* **19**: 5–9.
- 733 **Li H. 2023.** Protein-to-genome alignment with miniprot. *Bioinformatics* **39**.
- 734 **Li D, Liu C-M, Luo R, Sadakane K, Lam T-W. 2015.** MEGAHIT: an ultra-fast single-node  
735 solution for large and complex metagenomics assembly via succinct de Bruijn graph.  
736 *Bioinformatics* **31**: 1674–1676.
- 737 **Lu C, Yu Z, Zhang J, Cao P, Tian H, Nevison C. 2022.** Century-long changes and drivers of  
738 soil nitrous oxide (N<sub>2</sub>O) emissions across the contiguous United States. *Global change biology*  
739 **28**: 2505–2524.
- 740 **Lynch M. 1991.** METHODS FOR THE ANALYSIS OF COMPARATIVE DATA IN  
741 EVOLUTIONARY BIOLOGY. *Evolution; international journal of organic evolution* **45**: 1065–

742 1080.

743 **Maitner B. 2023.** *RBIEN: Tools for accessing the Botanical Information and Ecology Network*  
744 *(BIEN) database.* Github.

745 **McCormick RF, Truong SK, Sreedasyam A, Jenkins J, Shu S, Sims D, Kennedy M,**  
746 **Amirebrahimi M, Weers BD, McKinley B, et al. 2018.** The Sorghum bicolor reference  
747 genome: improved assembly, gene annotations, a transcriptome atlas, and signatures of genome  
748 organization. *The Plant journal: for cell and molecular biology* **93**: 338–354.

749 **McNear DH Jr. 2013.** The Rhizosphere - Roots, Soil and Everything In Between. *Nature*  
750 *Education Knowledge* **4**: 1.

751 **Miranda KM, Espey MG, Wink DA. 2001.** A rapid, simple spectrophotometric method for  
752 simultaneous detection of nitrate and nitrite. *Nitric oxide: biology and chemistry / official journal*  
753 *of the Nitric Oxide Society* **5**: 62–71.

754 **Mitros T, Session AM, James BT, Wu GA, Belaffif MB, Clark LV, Shu S, Dong H, Barling**  
755 **A, Holmes JR, et al. 2020.** Genome biology of the paleotetraploid perennial biomass crop  
756 *Miscanthus.* *Nature communications* **11**: 5442.

757 **Moore NA, Camac JS, Morgan JW. 2019.** Effects of drought and fire on resprouting capacity  
758 of 52 temperate Australian perennial native grasses. *The New phytologist* **221**: 1424–1433.

759 **Nuñez J, Arevalo A, Karwat H, Egenolf K, Miles J, Chirinda N, Cadisch G, Rasche F, Rao**  
760 **I, Subbarao G, et al. 2018.** Biological nitrification inhibition activity in a soil-grown biparental  
761 population of the forage grass, *Brachiaria humidicola.* *Plant and soil* **426**: 401–411.

762 **Otaka J, Subbarao GV, Ono H, Yoshihashi T. 2022.** Biological nitrification inhibition in  
763 maize—isolation and identification of hydrophobic inhibitors from root exudates. *Biology and*  
764 *fertility of soils* **58**: 251–264.

765 **Pan Z, Bajsa-Hirschel J, Vaughn JN, Rimando AM, Baerson SR, Duke SO. 2021.** In vivo  
766 assembly of the sorgoleone biosynthetic pathway and its impact on agroinfiltrated leaves of  
767 *Nicotiana benthamiana.* *The New phytologist* **230**: 683–697.

- 768 **Pariasca Tanaka J, Nardi P, Wissuwa M. 2010.** Nitrification inhibition activity, a novel trait in  
769 root exudates of rice. *AoB plants* **2010**: lq014.
- 770 **Parkin TB, Kaspar TC, Jaynes DB, Moorman TB. 2016.** Rye cover crop effects on direct and  
771 indirect nitrous oxide emissions. *Soil Science Society of America journal. Soil Science Society of*  
772 *America* **80**: 1551–1559.
- 773 **Patro R, Duggal G, Love MI, Irizarry RA, Kingsford C. 2017.** Salmon provides fast and bias-  
774 aware quantification of transcript expression. *Nature methods* **14**: 417–419.
- 775 **Petroli CD, Subbarao GV, Burgueño JA, Yoshihashi T, Li H, Franco Duran J, Pixley KV.**  
776 **2023.** Genetic variation among elite inbred lines suggests potential to breed for BNI-capacity in  
777 maize. *Scientific reports* **13**: 13422.
- 778 **Przybylska MS, Violle C, Vile D, Scheepens JF, Munoz F, Tenllado Á, Vinyeta M, Le Roux**  
779 **X, Vasseur F. 2024.** Can plants build their niche through modulation of soil microbial activities  
780 linked with nitrogen cycling? A test with *Arabidopsis thaliana*. *The New phytologist*.
- 781 **Rabalais NN, Turner RE. 2019.** Gulf of Mexico hypoxia: Past, present, and future. *Limnology*  
782 *and Oceanography Bulletin* **28**: 117–124.
- 783 **Rogovska N, O'Brien PL, Malone R, Emmett B, Kovar JL, Jaynes D, Kaspar T, Moorman**  
784 **TB, Kyveryga P. 2023.** Long-term conservation practices reduce nitrate leaching while  
785 maintaining yields in tile-drained Midwestern soils. *Agricultural water management* **288**:  
786 108481.
- 787 **Rossiter-Rachor NA, Setterfield SA, Douglas MM, Hutley LB, Cook GD, Schmidt S. 2009.**  
788 Invasive *Andropogon gayanus* (gamba grass) is an ecosystem transformer of nitrogen relations in  
789 Australian savanna. *Ecological applications: a publication of the Ecological Society of America*  
790 **19**: 1546–1560.
- 791 **Ross CW, Prihodko L, Anchang J, Kumar S, Ji W, Hanan NP. 2018.** HYSOGs250m, global  
792 gridded hydrologic soil groups for curve-number-based runoff modeling. *Scientific data* **5**:  
793 180091.

- 794 **Sarma AD, Sreelakshmi Y, Sharma R. 1997.** Antioxidant ability of anthocyanins against  
795 ascorbic acid oxidation. *Phytochemistry* **45**: 671–674.
- 796 **Schlesinger WH. 2009.** On the fate of anthropogenic nitrogen. *Proceedings of the National*  
797 *Academy of Sciences of the United States of America* **106**: 203–208.
- 798 **Schulz AJ, Zhai J, AuBuchon-Elder T, El-Walid M, Ferebee TH, Gilmore EH, Hufford**  
799 **MB, Johnson LC, Kellogg EA, La T, et al. 2023.** Fishing for a reelGene: evaluating gene  
800 models with evolution and machine learning. *bioRxiv*: 2023.09.19.558246.
- 801 **Shangguan W, Dai Y, Duan Q, Liu B, Yuan H. 2014.** A global soil data set for earth system  
802 modeling. *Journal of advances in modeling earth systems* **6**: 249–263.
- 803 **Smith C, Hill AK, Torrente-Murciano L. 2020.** Current and future role of Haber–Bosch  
804 ammonia in a carbon-free energy landscape. *Energy & environmental science* **13**: 331–344.
- 805 **Srikanthasamy T, Leloup J, N’Dri AB, Barot S, Gervais J, Koné AW, Koffi KF, Le Roux**  
806 **X, Raynaud X, Lata J-C. 2018.** Contrasting effects of grasses and trees on microbial N-cycling  
807 in an African humid savanna. *Soil biology & biochemistry* **117**: 153–163.
- 808 **Stamatakis A. 2014.** RAxML version 8: a tool for phylogenetic analysis and post-analysis of  
809 large phylogenies. *Bioinformatics* **30**: 1312–1313.
- 810 **Subbarao GV, Kishii M, Bozal-Leorri A, Ortiz-Monasterio I, Gao X, Ibba MI, Karwat H,**  
811 **Gonzalez-Moro MB, Gonzalez-Murua C, Yoshihashi T, et al. 2021.** Enlisting wild grass  
812 genes to combat nitrification in wheat farming: A nature-based solution. *Proceedings of the*  
813 *National Academy of Sciences of the United States of America* **118**: e2106595118.
- 814 **Subbarao GV, Nakahara K, Hurtado MP, Ono H, Moreta DE, Salcedo AF, Yoshihashi AT,**  
815 **Ishikawa T, Ishitani M, Ohnishi-Kameyama M, et al. 2009.** Evidence for biological  
816 nitrification inhibition in *Brachiaria* pastures. *Proceedings of the National Academy of Sciences*  
817 *of the United States of America* **106**: 17302–17307.
- 818 **Subbarao GV, Nakahara K, Ishikawa T, Ono H, Yoshida M, Yoshihashi T, Zhu Y, Zakir**  
819 **HAKM, Deshpande SP, Hash CT, et al. 2013.** Biological nitrification inhibition (BNI) activity

- 820 in sorghum and its characterization. *Plant and soil* **366**: 243–259.
- 821 **Subbarao GV, Rondon M, Ito O, Ishikawa T, Rao IM, Nakahara K, Lascano C, Berry WL.**  
822 **2007a.** Biological nitrification inhibition (BNI)—is it a widespread phenomenon? *Plant and soil*  
823 **294**: 5–18.
- 824 **Subbarao GV, Searchinger TD. 2021.** A ‘more ammonium solution’ to mitigate nitrogen  
825 pollution and boost crop yields. *Proceedings of the National Academy of Sciences* **118**:  
826 e2107576118.
- 827 **Subbarao GV, Tomohiro B, Masahiro K, Osamu I, Samejima H, Wang HY, Pearse SJ,**  
828 **Gopalakrishnan S, Nakahara K, Zakir Hossain AKM, et al. 2007b.** Can biological  
829 nitrification inhibition (BNI) genes from perennial *Leymus racemosus* (Triticeae) combat  
830 nitrification in wheat farming? *Plant and soil* **299**: 55–64.
- 831 **Subbarao GV, Wang HY, Ito O, Nakahara K, Berry WL. 2007c.** NH<sub>4</sub><sup>+</sup> triggers the synthesis  
832 and release of biological nitrification inhibition compounds in *Brachiaria humidicola* roots. *Plant*  
833 *and soil* **290**: 245–257.
- 834 **Sun L, Lu Y, Yu F, Kronzucker HJ, Shi W. 2016.** Biological nitrification inhibition by rice  
835 root exudates and its relationship with nitrogen-use efficiency. *The New phytologist* **212**: 646–  
836 656.
- 837 **Sun G, Wase N, Shu S, Jenkins J, Zhou B, Torres-Rodríguez JV, Chen C, Sandor L, Plott**  
838 **C, Yoshinga Y, et al. 2022.** Genome of *Paspalum vaginatum* and the role of trehalose mediated  
839 autophagy in increasing maize biomass. *Nature communications* **13**: 7731.
- 840 **Sun S, Zhou Y, Chen J, Shi J, Zhao H, Zhao H, Song W, Zhang M, Cui Y, Dong X, et al.**  
841 **2018.** Extensive intraspecific gene order and gene structural variations between Mo17 and other  
842 maize genomes. *Nature genetics* **50**: 1289–1295.
- 843 **Tesfamariam T, Yoshinaga H, Deshpande SP, Srinivasa Rao P, Sahrawat KL, Ando Y,**  
844 **Nakahara K, Hash CT, Subbarao GV. 2014.** Biological nitrification inhibition in sorghum: the  
845 role of sorgoleone production. *Plant and soil* **379**: 325–335.

- 846 **Villegas D, Arevalo A, Nuñez J, Mazabel J, Subbarao G, Rao I, De Vega J, Arango J. 2020.**  
847 Biological Nitrification Inhibition (BNI): Phenotyping of a Core Germplasm Collection of the  
848 Tropical Forage Grass *Megathyrsus maximus* Under Greenhouse Conditions. *Frontiers in plant*  
849 *science* **11**: 820.
- 850 **Wang X, Li Z, Policarpio L, Koffas MAG, Zhang H. 2020.** De novo biosynthesis of complex  
851 natural product sakuranetin using modular co-culture engineering. *Applied microbiology and*  
852 *biotechnology* **104**: 4849–4861.
- 853 **Wang G, Zhang L, Guo Z, Shi D, Zhai H, Yao Y, Yang T, Xin S, Cui H, Li J, et al. 2023.**  
854 Benefits of biological nitrification inhibition of *Leymus chinensis* under alkaline stress: the  
855 regulatory function of ammonium-N exceeds its nutritional function. *Frontiers in plant science*  
856 **14**: 1145830.
- 857 **Widhalm JR, Rhodes D. 2016.** Biosynthesis and molecular actions of specialized 1,4-  
858 naphthoquinone natural products produced by horticultural plants. *Horticulture research* **3**:  
859 16046.
- 860 **Zhang M, Gao X, Chen G, Afzal MR, Wei T, Zeng H, Subbarao GV, Wei Z, Zhu Y. 2023.**  
861 Intercropping with BNI-sorghum benefits neighbouring maize productivity and mitigates soil  
862 nitrification and N<sub>2</sub>O emission. *Agriculture, ecosystems & environment* **352**: 108510.
- 863 **Zhang T, Huang W, Zhang L, Li D-Z, Qi J, Ma H. 2024.** Phylogenomic profiles of whole-  
864 genome duplications in Poaceae and landscape of differential duplicate retention and losses  
865 among major Poaceae lineages. *Nature communications* **15**: 3305.
- 866